

# Colored Resonances at the Tevatron: Phenomenology and Discovery Potential in Multijets

---

Can Kilic<sup>(a)</sup>, Takemichi Okui<sup>(a,b)</sup> and Raman Sundrum<sup>(a)</sup>

*(a) Department of Physics and Astronomy, Johns Hopkins University,  
Baltimore, MD 21218, USA*

*(b) Department of Physics, University of Maryland,  
College Park, MD 20742, USA*

**ABSTRACT:** There exist several classes of theories beyond the Standard Model which contain massive spin-1 color octets, generically called “colorons”. Indeed we argue that colorons inevitably appear in the spectrum whenever new colored particles feel an additional confining force. Colorons are distinctive at hadron colliders as this is the only environment in which they can be resonantly produced. In the simplest models we show that the coloron naturally decays to multijets via secondary resonances, which can be consistent with all existing bounds, even for colorons as light as a few hundred GeV. We perform representative case studies and show that a search in the four-jet channel at the Tevatron has strong signal significance, while the LHC faces formidable challenges for such a search.

**KEYWORDS:** Jets, Beyond Standard Model, Hadronic Colliders, Phenomenological Models.

## 1. Introduction and the Scenario

Hadron colliders such as the Tevatron and LHC are ideal for producing new colored particles with weak-scale masses. Such particles may be associated with mechanisms for resolving the Hierarchy Problem, such as Supersymmetry, Strong Dynamics, Extra Dimensions, or Little Higgs, or they may arise for other seemingly incidental reasons (as did the second and third generation quarks). The standard strategy for discovery of such states is to take advantage of QCD cross sections for their *pair-production*, and to exploit their electroweak or other distinctive interactions in order to pull them out of the enormous QCD backgrounds. New electroweak and/or flavor physics is however strongly constrained by a host of precision data, which hints that such new states are relatively heavy. A different possibility arises if there is a new colored particle with the same quantum numbers as the gluon, a color-octet massive vector boson, which can then be produced *resonantly* via mixing with a virtual *s*-channel gluon. One can then hope to pick out such a sizable resonance from the non-resonant QCD backgrounds, even without relying on flavor-tagged, leptonic, or missing energy signatures.

Indeed color octet vector particles have appeared in new physics proposals in various guises: massive gauge bosons from extensions of QCD gauge structure in Topcolor models [1], Kaluza-Klein excited gluons in extra-dimensional models, composite colored vector mesons in non-minimal Technicolor [2], and string excitations of the gluon in TeV Gravity [3]. We will borrow the terminology of Refs. [1, 4] and refer to any such massive vector particle as a “coloron”.

Colorons can also arise rather minimally, apart from the dramatic scenarios cited above. Imagine QCD pair-production of a *new* colored particle and its anti-particle via *s*-channel gluon exchange, but where the pair are bound together with a new stronger force. The bound state is then necessarily a coloron! This is highly plausible given the prevalence of confinement among non-abelian gauge theories. In fact, Nature has given us a useful precedent in QED and hadronic physics. A virtual photon from electron-positron annihilation can pair-produce new charged particles and anti-particles. When the new particles happen to be quarks, the strong interactions can confine the quark and anti-quark pair into a single resonance, the  $\rho$ , emerging from the virtual photon. In hadronic physics this is referred to as “photon- $\rho$  mixing”.<sup>1</sup>

Our viewpoint is that the coloron is an object of general phenomenological interest, much like a  $Z'$ , readily produced and with diverse theoretical motivations, and that search strategies should be devised to cover the promising signatures. In this paper, we point out that there is a sizable regime, which is not excluded by existing data, where a coloron can be discovered in multi-jet studies at the Tevatron, which is however *much more difficult to find at the LHC*. Discovery does not require the new physics to carry electroweak or

---

<sup>1</sup>To be clear then, in this analogy the role of the virtual gluon created by a  $q\bar{q}$  pair is played by a virtual photon created by an  $e^+e^-$  pair, the role of the composite coloron is played by the composite  $\rho$  meson, and the role of a new weak-scale strong force holding the coloron together is played by the ordinary GeV-scale strong interactions of QCD holding the  $\rho$  together.

flavor quantum numbers, and therefore the Tevatron accessibility is not necessarily in conflict with precision data. In this paper this is naturally achieved by having the quarks couple to the coloron only via gluon-coloron mixing. Stronger flavor blind quark-coloron couplings have been proposed earlier in [4], however this scenario is excluded in the sub-TeV regime which is our focus [5, 6]. While precision constraints do allow the coloron to couple strongly to the top quark [7, 8] ( $t_R$  in particular), at Tevatron energies this is severely constrained by measurements of the top production cross section. Ref. [9] studied the early Tevatron implications of a phenomenological model containing a coloron with an adjustable coupling to the top quark. For the LHC phenomenology of heavier colorons with strong top coupling, see Refs. [10, 11, 12].

In fact the most severe constraints come, not from electroweak or flavor tests, but from past dijet studies [13, 14, 15]. A coloron, once produced, can decay by mixing back into a virtual gluon and then into  $q\bar{q}$ , thereby creating a dijet resonance. If this channel dominated the decay of the coloron, then most of the sub-TeV mass range is already excluded (for a “typical” size of gluon-coloron mixing, to be discussed shortly). However, looking at it more closely this is not what the QED analogy with the  $\rho$  meson suggests. Notice that  $\rho \rightarrow e^+e^-$  is *not* the dominant decay mode of  $\rho$  at all; it is  $\rho \rightarrow \pi\pi$  that is nearly 100%. Translated to the case of interest, the coloron can naturally decay dominantly into other new colored resonances, which may in turn decay into several jets, thereby diminishing the dijet decays of the coloron below existing bounds. The coloron effectively becomes a multi-jet resonance. The purpose of this paper is to study the phenomenology of the coloron and secondary resonances in multi-jet processes.

The paper is organized as follows: In section 2 we write down a simple and renormalizable theory of a coloron and a secondary resonance realized as bound states of new strong dynamics in close analogy to hadronic physics. In section 3 we introduce a phenomenological Lagrangian for this theory capturing the production of the coloron as well as subsequent decays. We will then show in section 4 that this benchmark model is consistent with existing constraints and in section 5 will lay out a search strategy for its discovery at the Tevatron for a range of coloron masses. We will conclude in section 6 with a discussion of our results and future prospects for alternative coloron models.

## 2. An Illustrative Model

The purpose of the following simple field theory model is to demonstrate how general the phenomenon of a coloron can be, that it can be decoupled from dangerous new electroweak or flavor effects, and to show that the coloron can readily have strong decay modes that dilute the dijet resonance channel, making it predominantly a multi-jet signal.

Consider the renormalizable theory given by

$$\mathcal{L} = \mathcal{L}_{\text{SM}} + \bar{\psi}(i\not{D} - m)\psi - \frac{1}{4}H_{\mu\nu}H^{\mu\nu}. \quad (2.1)$$

The second term simply describes the addition of some new color-triplet Dirac fermions, such as we might contemplate pair-producing at a hadron collider. For maximal safety in precision tests let us take them to be electroweak singlets with no connection to standard-model (SM) flavor. In addition we assume that the new fermions transform under a new non-abelian gauge group, “hyper-color” (HC), described by the third term above, which is confining at a scale  $\Lambda_{\text{HC}}$ . New confining forces, in particular modeled on QCD, play a role in a number of other phenomenologically interesting scenarios beyond the SM, such as Technicolor [16] and its variants, “hidden valley” [17], or “quirk” models [18].

Our analysis will be relevant when  $\Lambda_{\text{HC}}$  is in the range of 100s of GeV, but it is not fundamentally constrained to that regime. Therefore, instead of pair-production of the new hyper-quarks we will have production of the  $\Lambda_{\text{HC}}$ -scale hyper-hadrons. We can in fact safely set the “current” mass to zero,  $m \rightarrow 0$ , and we do so from now on for simplicity.

The fact that the new particles are all flavor and electroweak “blind” ensures their safety for most precision tests. (There is a blind precision test however, the tests of quark “compositeness” effects, that will be treated separately in section 4.) The real meaning behind the technical renormalizability of the model is that there can be a separation of scales between  $\Lambda_{\text{HC}}$  and yet other new physics. Such new physics may have electroweak and flavor components, and may address the hierarchy problem, but it does not have to interfere with the lower-energy physics of the HC sector.

For convenience, we take HC to mimic QCD structure as much as possible so that we can translate strong-interaction matrix elements directly from their measured QCD values to the HC physics, with the simple rescaling  $\Lambda_{\text{QCD}} \rightarrow \Lambda_{\text{HC}}$ . We therefore take the HC gauge group to be  $\text{SU}(3)_{\text{HC}}$ , with three massless flavors,  $\psi$ , and therefore  $\text{SU}(3)$  flavor symmetry. This is just a rescaled version of QCD with three light flavors, without current masses or electroweak charges. An important difference is that while QCD’s flavor symmetry is weakly gauged, but only partially, by electromagnetism, HC’s flavor symmetry will be completely gauged by QCD itself (which is weak at  $\Lambda_{\text{HC}}$  energies). That is, we are identifying HC flavor symmetry with QCD gauge symmetry, thus taking our Dirac fermions,  $\psi$ , to be bi-fundamentals  $(\mathbf{3}, \bar{\mathbf{3}})$  of  $\text{SU}(3)_{\text{QCD}} \times \text{SU}(3)_{\text{HC}}$ .

We can therefore automatically estimate the spectrum of the HC sector by just rescaling the ordinary hadronic spectrum. In particular, we know that there is an  $\text{SU}(3)$  flavor octet of massive vector mesons imitating the ordinary  $\rho$  (and its flavor siblings). Since the  $\text{SU}(3)$  flavor symmetry of the hyper-hadrons is identified with  $\text{SU}(3)_{\text{QCD}}$ , this is precisely a QCD octet “coloron”, which is created by the QCD color current (virtual gluon) just as the  $\rho^0$  is created by the electromagnetic current (virtual photon). The coloron mass is of order  $\Lambda_{\text{HC}}$ , and we can just use  $m_{\text{coloron}}$  as our unit of measure rather than  $\Lambda_{\text{HC}}$ . The coloron is not the lightest hyper-hadron however, there must be a QCD octet hyper-pion, which is lighter than the coloron, being a (pseudo-)Goldstone multiplet of the HC dynamics, as we will see more explicitly below. In particular the coloron can decay into a hyper-pion pair. While there will be a host of heavier hyper-hadrons they will not be relevant for our analysis or Tevatron studies. They may however be interesting for the LHC.

Non-minimal technicolor models [2] also contain a coloron with a colored techni-pion decay mode. Ref. [19] considered the SSC phenomenology of techni-pion production but found the coloron resonance relatively uninteresting. Ref. [20] devoted to walking technicolor phenomenology took the couplings for coloron decay to techni-pions to be insignificant. Ref. [21] studied coloron production and techni-pion decays at the Tevatron, but focussed on a signal with a photon in the final state, which was found not to be significant enough for discovery.

### 3. The Phenomenological Lagrangian

At the kind of precision and energy at the Tevatron, we can approximate the complexity of the full HC dynamics by simple effective vertices for the coloron,  $\tilde{\rho}$ , and hyper-pion,  $\tilde{\pi}$ , as well as their couplings to QCD, sufficient to describe their production and decays. We can then fit the couplings of the effective vertices by matching them to the analogous vertices describing the ordinary  $\rho$  and  $\pi$  mesons and their couplings to QED, which can be extracted from hadronic data.

Omitting the electroweak-Higgs sector and the leptons, our effective Lagrangian is given by

$$\begin{aligned}
\mathcal{L}_{\text{eff}}^{\text{HC}} = & \bar{q}i\tilde{D}q - \frac{1}{4}G_{\mu\nu}^a G^{a\mu\nu} \\
& - \frac{1}{4}\tilde{\rho}_{\mu\nu}^a \tilde{\rho}^{a\mu\nu} + \frac{m_{\tilde{\rho}}^2}{2}\tilde{\rho}_\mu^a \tilde{\rho}^{a\mu} + \frac{\tilde{\varepsilon}}{2}\tilde{\rho}_{\mu\nu}^a G^{a\mu\nu} \\
& + \frac{1}{2}(\tilde{D}_\mu \tilde{\pi})^a (\tilde{D}^\mu \tilde{\pi})^a - \frac{m_{\tilde{\pi}}^2}{2}\tilde{\pi}^a \tilde{\pi}^a \\
& - g_{\tilde{\rho}\tilde{\pi}\tilde{\pi}} f^{abc} \tilde{\rho}_\mu^a \tilde{\pi}^b \tilde{D}^\mu \tilde{\pi}^c - \frac{3g_3^2 \epsilon^{\mu\nu\rho\sigma}}{16\pi^2 f_{\tilde{\pi}}} \text{tr}[\tilde{\pi}^a T^a G_{\mu\nu} G_{\rho\sigma}].
\end{aligned} \tag{3.1}$$

Here, the indices  $a, b, c$  run from 1 through 8, labelling the eight states of the color octet.  $\tilde{D}_\mu$  denotes the covariant derivative containing a gluon field, and the reason for the tilde will become clear shortly. The first line above describes the kinetic terms for the standard-model quark  $q$  and the gluon  $G_{\mu\nu} = G_{\mu\nu}^a T^a$ , with the SU(3) generators  $T^a$ . The second line contains the kinetic and mass terms for the coloron, where  $\tilde{\rho}_{\mu\nu} \equiv \tilde{D}_\mu \tilde{\rho}_\nu - \tilde{D}_\nu \tilde{\rho}_\mu$ , and the gluon-coloron mixing parameterized by  $\tilde{\varepsilon}$ . The third line describes the kinetic and mass terms for the hyper-pions. The fourth line describes the  $\tilde{\rho} \rightarrow \tilde{\pi}\tilde{\pi}$  decay and the  $\tilde{\pi} \rightarrow gg$  decay.

Now, note that the above phenomenological Lagrangian has a close analog in Nature:

$$\begin{aligned}
\mathcal{L}_{\text{eff}}^{\text{QCD}} = & \bar{e}iD e - \frac{1}{4}F_{\mu\nu} F^{\mu\nu} \\
& - \frac{1}{4}\rho_{\mu\nu} \rho^{\mu\nu} + \frac{m_\rho^2}{2}\rho_\mu \rho^\mu + \frac{\varepsilon}{2}\rho_{\mu\nu} F^{\mu\nu} \\
& + \frac{1}{2}\partial_\mu \pi^0 \partial^\mu \pi^0 - m_{\pi^0}^2 \pi^0 \pi^0 \\
& + D_\mu \pi^- D^\mu \pi^+ - m_{\pi^\pm}^2 \pi^- \pi^+ \\
& - ig_{\rho\pi\pi} \rho^\mu (\pi^- \overleftrightarrow{D}_\mu \pi^+) - \frac{e^2 \epsilon^{\mu\nu\rho\sigma}}{32\pi^2 f_\pi} \pi^0 F_{\mu\nu} F_{\rho\sigma},
\end{aligned} \tag{3.2}$$

where  $A\overleftrightarrow{\partial}B \equiv A\partial B - (\partial A)B$ . Here,  $D_\mu$  denotes the covariant derivative containing a photon, and the absence of the tilde distinguishes it from  $\tilde{D}_\mu$ . The first line describes the kinetic terms for the electron and the photon, while the second line contains the kinetic and mass terms for the neutral  $\rho$  meson, where  $\rho_{\mu\nu} \equiv \partial_\mu\rho_\nu - \partial_\nu\rho_\mu$ , and the photon- $\rho$  mixing parameterized by  $\varepsilon$ . The third and fourth lines describe the kinetic and mass terms for the neutral and charged pions, and finally the fifth line describes the  $\rho \rightarrow \pi^+\pi^-$  decay and the  $\pi^0 \rightarrow \gamma\gamma$  decay. (Note that  $f_{\tilde{\pi}}$  and  $f_\pi$  are normalized in the same way.)

Now, let us translate carefully between (3.1) and (3.2) to extract the parameters in (3.1) from (3.2). First, there is a straightforward change of the scale, from  $\Lambda_{\text{QCD}} \sim m_\rho$  to  $\Lambda_{\text{HC}} \sim m_{\tilde{\rho}}$ . This immediately implies that  $f_\pi \simeq 92 \text{ MeV}$  is translated to

$$f_{\tilde{\pi}} \simeq 92 \text{ GeV} \frac{m_{\tilde{\rho}}}{10^3 m_\rho}, \quad (3.3)$$

although the precise value of  $f_{\tilde{\pi}}$  is not important for our phenomenology, since all we need to know is that  $\tilde{\pi}$  decays promptly.

We now turn to  $g_{\tilde{\rho}\tilde{\pi}\tilde{\pi}}$ . Since QCD is a small perturbation to the hyper-color dynamics just like QED is a small perturbation to the color dynamics, we expect that  $g_{\tilde{\rho}\tilde{\pi}\tilde{\pi}} = g_{\rho\pi\pi}$  as the decay  $\rho \rightarrow \pi^+\pi^-$  is governed by the strong interactions. All we need to check is the normalization conventions, for which considering the entire octet of the mesons is useful:

$$f^{abc} \rho_\mu^a \pi^b \partial^\mu \pi^c = i \rho^\mu (\pi^- \overleftrightarrow{\partial}_\mu \pi^+) + \dots, \quad (3.4)$$

which shows  $g_{\tilde{\rho}\tilde{\pi}\tilde{\pi}}$  and  $g_{\rho\pi\pi}$  are normalized in the same way. Thus, we have

$$g_{\tilde{\rho}\tilde{\pi}\tilde{\pi}} = g_{\rho\pi\pi} \simeq 6, \quad (3.5)$$

which is extracted by using (3.2) to fit  $\Gamma_{\rho \rightarrow \pi\pi} = 149 \text{ MeV}$ . As we will show in the next section, this strong coupling puts us significantly below any dijet bounds.

Next, to make the  $\tilde{\rho}$ - $q$ - $\bar{q}$  coupling explicit, we redefine the gluon field as  $G_\mu^a \rightarrow G_\mu^a + \tilde{\varepsilon} \tilde{\rho}_\mu^a$ . Neglecting  $O(\tilde{\varepsilon}^2)$ , this eliminates the  $\tilde{\varepsilon}$  term in the second line of (3.1). However, the shift also affects  $\bar{q}i\overleftrightarrow{\not{D}}q$ , and the following new term now appears in (3.1):

$$\mathcal{L}_{\tilde{\rho}q\bar{q}} = -g_3 \tilde{\varepsilon} \tilde{\rho}_\mu^a \bar{q} \gamma^\mu T^a q, \quad (3.6)$$

which describes the coloron production from a  $q$ - $\bar{q}$  collision and its decay into a dijet. To determine the value of  $\tilde{\varepsilon}$ , we perform the analogous shift in (3.2), which induces the  $\rho$ - $e^+e^-$  coupling  $-e\varepsilon\rho_\mu\bar{e}\gamma^\mu e$ . Using this to fit the partial width  $\Gamma_{\rho \rightarrow e^+e^-} = 7.04 \text{ keV}$  gives  $\varepsilon \simeq 0.06$ . To translate this to  $\tilde{\varepsilon}$ , notice that the  $\rho$ - $\gamma$  mixing parameter  $\varepsilon$  itself is proportional to the gauge coupling  $e$ , because ‘‘microscopically’’ it is the quark-antiquark pair inside the  $\rho$  annihilating into the (off-shell) photon. Thus, the  $\tilde{\varepsilon}$  must be rescaled by the ratio of the gauge couplings:

$$\tilde{\varepsilon} = \frac{g_3}{e} \varepsilon \simeq 0.2, \quad (3.7)$$

The last parameter to be extracted is  $m_{\tilde{\pi}}$ . Note that the hyper-pions  $\tilde{\pi}$  would be exact Goldstone bosons if  $g_3$  were zero. The corresponding statement in the analog (3.2) is that the mass-squared *difference* between the charged and the neutral pions would be zero if  $e$  were zero (up to small corrections of  $O(m_{u,d}^2)$ ). Therefore we can use chiral perturbation theory to extrapolate the mass of the hyper-pion from the pion mass difference. We find

$$\frac{m_{\tilde{\pi}}^2}{m_{\tilde{\rho}}^2} = 3 \frac{g_3^2}{e^2} \frac{m_{\pi^\pm}^2 - m_{\pi^0}^2}{m_{\rho}^2} \quad (3.8)$$

where we have included the color factor. Numerically this gives

$$m_{\tilde{\pi}} \simeq 0.3m_{\tilde{\rho}}. \quad (3.9)$$

To summarize, we will in the rest of the paper use the effective Lagrangian

$$\begin{aligned} \mathcal{L}_{\text{eff}}^{\text{HC}} = & \bar{q}i\tilde{D}q - g_3\tilde{\varepsilon}\rho_\mu^a\bar{q}\gamma^\mu T^a q \\ & - \frac{1}{4}G_{\mu\nu}^a G^{a\mu\nu} - \frac{1}{4}\tilde{\rho}_{\mu\nu}^a \tilde{\rho}^{a\mu\nu} + \frac{m_{\tilde{\rho}}^2}{2}\tilde{\rho}_\mu^a \tilde{\rho}^{a\mu} \\ & + \frac{1}{2}(\tilde{D}_\mu\tilde{\pi})^a (\tilde{D}^\mu\tilde{\pi})^a - \frac{m_{\tilde{\pi}}^2}{2}\tilde{\pi}^a \tilde{\pi}^a \\ & - g_{\tilde{\rho}\tilde{\pi}\tilde{\pi}} f^{abc}\tilde{\rho}_\mu^a \tilde{\pi}^b \partial^\mu \tilde{\pi}^c - \frac{3g_3^2\epsilon^{\mu\nu\rho\sigma}}{16\pi^2 f_{\tilde{\pi}}}\text{tr}[\tilde{\pi}^a T^a G_{\mu\nu} G_{\rho\sigma}], \end{aligned} \quad (3.10)$$

where  $f_{\tilde{\pi}}$ ,  $g_{\tilde{\rho}\tilde{\pi}\tilde{\pi}}$ ,  $\tilde{\varepsilon}$ , and  $m_{\tilde{\pi}}$  are given by (3.3), (3.5), (3.7), and (3.9), this will be referred to as “the benchmark model”. Note that in the benchmark model  $m_{\tilde{\rho}}$  is the only free parameter. In this paper we will restrict ourselves to a range for  $m_{\tilde{\rho}}$  which makes the coloron discoverable at the Tevatron. We will elaborate further on this in our conclusions. A case study for the discovery potential will be presented in section 5 with a strong result.

We should mention at this point that while it is not possible to resonantly produce a coloron from a gluon-gluon initial state through renormalizable operators, there are higher dimensional operators which can do this, the leading one being  $(\alpha_s/m_{\tilde{\rho}}^2)f^{abc}\tilde{\rho}_\nu^{a\mu}G_\mu^{b\sigma}G_\sigma^{c\nu}$ , using naive dimensional analysis [22, 23] for the strong hypercolor interactions. However, the effect of this operator on resonant coloron production is negligible at the Tevatron since the coupling to  $q\bar{q}$  combined with valence quark PDF’s completely dominates the cross section (so that a more precise estimate of the coefficient of the above operator is unnecessary).

As we have alluded to in the introduction, in the benchmark model the dominant decay mode of the coloron is into a pair of hyper-pions, and the branching fraction into quarks is suppressed by the mixing of the coloron with the gluon, which is the reason why this model is not in conflict with the dijet resonance bounds from the Tevatron. This will be explained in detail in section 4. In figure 1 we plot the branching fractions of the coloron as a function of its mass, calculated using COMPHEP4.4 [24].

It should be kept in mind that while the parameters appearing in Eq. (3.10) are ultimately determined by the theory in Eq. (2.1), one can easily imagine that alternate fundamental

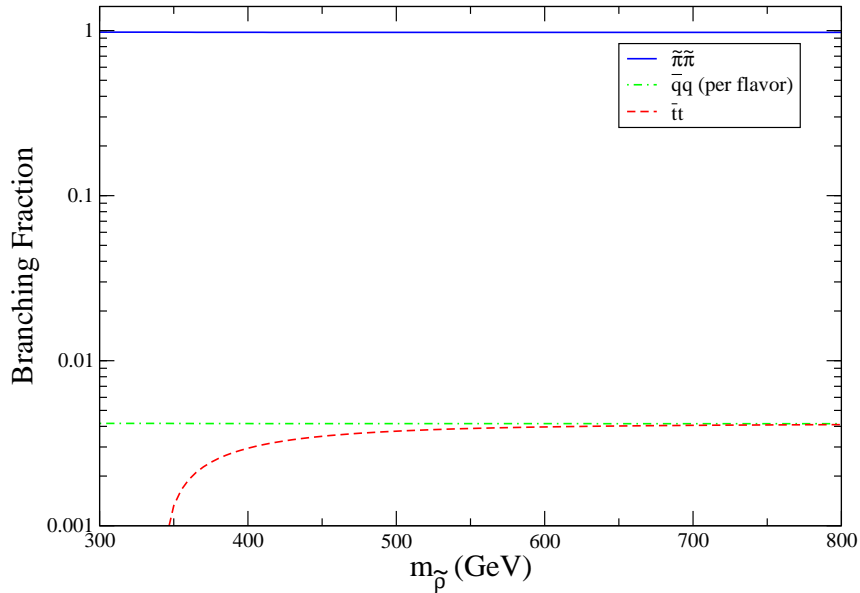


**Figure 1:** The branching fractions of the coloron as a function of its mass in the benchmark model.

dynamics can lead to different values for these parameters. Physically  $\tilde{\epsilon}$  sets the overall production cross section of the coloron, while the ratio  $\tilde{\epsilon}/g_{\tilde{\rho}\tilde{\pi}\tilde{\pi}}$  sets the ratio of the partial decay widths  $\Gamma_{\tilde{\rho}\rightarrow q\bar{q}}/\Gamma_{\tilde{\rho}\rightarrow\tilde{\pi}\tilde{\pi}}$ . In section 4 we will quantitatively relate the constraints on the benchmark model to these effective parameters, as well as  $m_{\tilde{\pi}}$ .

## 4. Constraints on the Benchmark Model

In this section we will go through various potential constraints on the benchmark model described in the previous section, and establish that our scenario is compatible with existing experimental bounds. The benchmark model, with  $g_{\tilde{\rho}\tilde{\pi}\tilde{\pi}}$  and  $m_{\tilde{\pi}}/m_{\tilde{\rho}}$  fixed, has only one free parameter, namely  $\Lambda_{\text{HC}}$  or equivalently  $m_{\tilde{\rho}}$ .

### 4.1 Constraints on the $\tilde{\rho}$ Particle

An obvious constraint on the coloron comes from resonance searches in the dijet channel. The most recent publicly available bounds on resonant dijet production are reported in [14] as well as [15] (for heavy flavor-tagged jets). We plot in figure 2 the dijet production cross section through the coloron (calculated using [24]) in the benchmark model as a function of  $m_{\tilde{\rho}}$  and compare to the bounds obtained by the CDF collaboration. We remark here that the exclusion curve has detector acceptance folded in (both jets are required to be central,



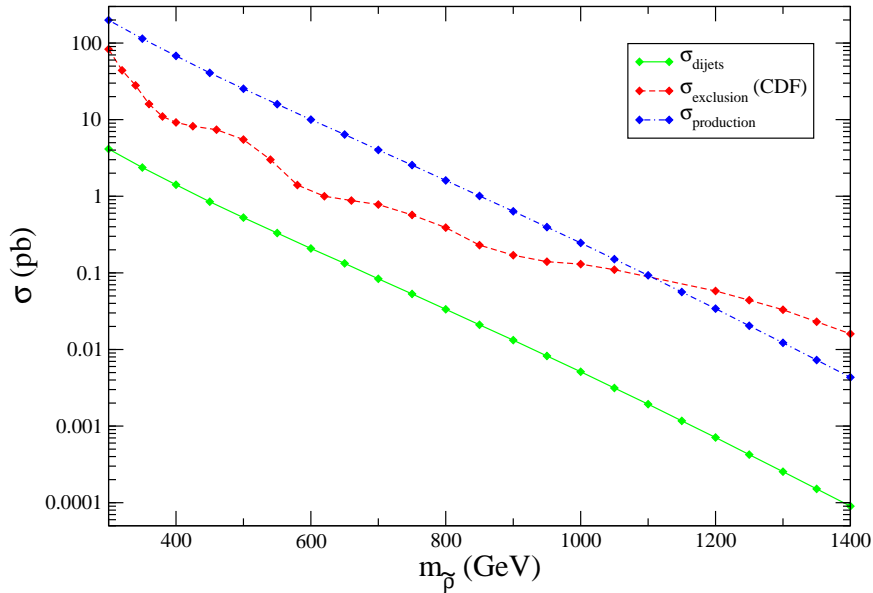


**Figure 2:** The comparison of our benchmark model with recent CDF exclusion bounds on dijet resonances. The green curve represents the cross section for dijet production through the coloron at Tevatron Run-II as a function of the coloron mass and the red curve represents the CDF dijet exclusion bound obtained from  $1.13 \text{ fb}^{-1}$  of data. In this plot signal is presented with perfect acceptance while the exclusion curve was obtained by demanding that both jets be central ( $|y^{\text{j}et1,2}| < 1$ ), thus in reality our benchmark model is even less constrained than this conservative plot suggests. For completeness we include the *total* production cross section of the coloron represented by the blue curve which illustrates that for the coloron not to be excluded, the smallness of the dijet branching fraction is crucial.

( $|y^{\text{j}et1,2}| < 1$ ) while for the signal we are plotting the cross section assuming perfect acceptance, hence this plot is overly conservative. We include in this plot the *total*  $\tilde{\rho}$  production cross section, note that for most choices of  $m_{\tilde{\rho}}$  the model would have been excluded if dijets were the dominant decay mode of the coloron. However, the presence of the  $\tilde{\pi}\text{-}\tilde{\pi}$  mode lowers the dijet production cross section significantly below the bound. A potential worry, namely that detector effects may cause a fraction of the four-jet signal events to be reconstructed as dijet events with the correct value of  $m_{\tilde{\rho}}$ , is disarmed by the fact that the total production cross section of the coloron is always within a factor of order one of the dijet bound.

The dijet bound is also the primary constraint for going beyond the benchmark model and varying the parameters of the phenomenological Lagrangian presented in (3.10). It is straightforward to verify that for a given value of  $m_{\tilde{\rho}}$  the dependence of the dijet cross section

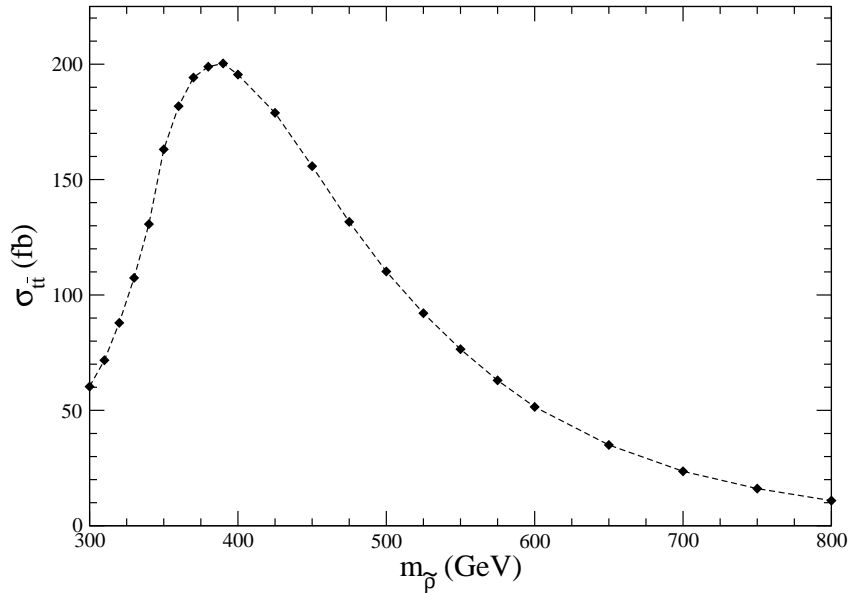


**Figure 3:**  $\sigma(pp \rightarrow \tilde{\rho} \rightarrow t\bar{t})$  cross section at Tevatron Run-II as a function of  $m_{\tilde{\rho}}$  for the benchmark model. For  $m_{\tilde{\rho}}$  near or below the  $t\bar{t}$  threshold, we plot the cross section with one of the  $t$ -quarks off-shell.

on the model parameters is given by

$$\sigma_{dijet} = (\sigma_0)_{dijet} \left( \frac{\tilde{\epsilon}}{\tilde{\epsilon}_0} \right)^4 \left( \frac{g_{\tilde{\rho}\tilde{\pi}\tilde{\pi},0}}{g_{\tilde{\rho}\tilde{\pi}\tilde{\pi}}} \right)^2 \left( \frac{m_{\tilde{\rho}}^2 - 4m_{\tilde{\pi},0}^2}{m_{\tilde{\rho}}^2 - 4m_{\tilde{\pi}}^2} \right)^{3/2} \quad (4.1)$$

(assuming  $\Gamma_{\tilde{\rho} \rightarrow q\bar{q}} \ll \Gamma_{\tilde{\rho} \rightarrow \tilde{\pi}\tilde{\pi}}$  still holds) where the subscripts 0 denote the parameters of the benchmark model. (For  $\Gamma_{\tilde{\rho} \rightarrow q\bar{q}} \gg \Gamma_{\tilde{\rho} \rightarrow \tilde{\pi}\tilde{\pi}}$ ,  $\sigma_{dijet} \sim \sigma_{prod}$ .) Thus, it is straightforward to use figure 2 to constrain the parameters of (3.10).

The  $t\bar{t}$  branching mode is another source of potential constraints on the  $\tilde{\rho}$  production cross section. In figure 3 we plot the  $t\bar{t}$  cross section via  $\tilde{\rho}$  production and decay as a function of  $m_{\tilde{\rho}}$  in the benchmark model (calculated using [24]). Note that the cross section stays below 0.2 pb for the entire range of  $m_{\tilde{\rho}}$ , which is below the lower bounds in [25]. Note that [25] searches for a *narrow* resonance that decays to a  $t\bar{t}$  pair, so the bound on a wide resonance such as our  $\tilde{\rho}$  is actually even weaker.

There are studies of multi-jet final states at Tevatron Run-I [26] which found no deviations from the QCD predictions, however these studies use large  $p_T$  and  $m_{inv}$  cuts such that the events coming from a light coloron ( $m_{\tilde{\rho}} < 500$  GeV) do not pass the analysis cuts while for a heavier coloron the cross section is low enough such that any excess produced is not

statistically significant. We have found  $m_{\tilde{\rho}} \sim 700$  GeV to be the point where the number of events passing the cuts used in [26] is maximized at roughly 60, which would correspond to a  $2\sigma$  excess in their distributions.

In our benchmark model, there is a three jet decay mode  $\tilde{\rho} \rightarrow g\tilde{\pi}$  for the coloron, which is the analogue of  $\rho \rightarrow \gamma\pi$  in QCD. Scaling up the partial width for this process from QCD using the appropriate factors ( $\frac{\alpha_s}{\alpha_{em}}$  for coupling constants and 3 for number of colors) we find that the relevant branching fraction is a few percent, so the number of three jet events from this decay mode should be similar to the number of dijet events. Ref. [26] is insensitive to such a low number of three jet events.

Finally, VISTA and SLEUTH global searches [27] have been performed to look for anomalies in the Tevatron data (with emphasis on high- $p_T$  deviations). As we will show in section 5 a blind global search has limited sensitivity to the presence of  $\tilde{\rho}$  while a more optimized search taking advantage of the presence of secondary resonances yields much stronger evidence for a discrepancy in kinematic distributions.

## 4.2 Constraints on the $\tilde{\pi}$ Particle

The  $\tilde{\pi}$  particle in the benchmark model has a coupling to a pair of gluons through the anomaly, and can thus be resonantly produced from a  $g$ - $g$  initial state. The  $\tilde{\pi}$  subsequently decays back to two gluons, so in principle one can observe the  $\tilde{\pi}$  as a narrow resonance in dijets. However, due to the loop factor in the effective vertex, the  $gg \rightarrow \tilde{\pi}$  cross section is strongly suppressed. At the parton level, averaging over colors and spins, we have

$$\frac{1}{2^2} \frac{1}{8^2} \sum_{\text{color,spin}} |\mathcal{M}_{gg \rightarrow \tilde{\pi}}|^2 = \frac{15\alpha_s^2}{256\pi^2} \frac{\hat{s}^2}{f_{\tilde{\pi}}^2}. \quad (4.2)$$

Since we consider values of  $m_{\tilde{\pi}}$  as low as 100 GeV we need to consider dijet resonance constraints from  $Spp\bar{S}$ . We integrate (4.2) using CTEQ5L PDF's [28] to calculate the  $\tilde{\pi}$  production cross section at a center of mass of 630 GeV and find  $\sigma(p\bar{p} \rightarrow \tilde{\pi}) \simeq 12$  pb for  $m_{\tilde{\pi}} = 100$  GeV and  $f_{\tilde{\pi}} = 43$  GeV (i.e.  $m_{\tilde{\rho}} = 350$  GeV), which is below the bound given in [13] (for an earlier phenomenological study of colored resonances at  $Spp\bar{S}$ , see [29]). Similarly we obtain for Tevatron Run-II  $\sigma(p\bar{p} \rightarrow \tilde{\pi}) \simeq 3.8$  pb for  $m_{\tilde{\pi}} = 250$  GeV and  $f_{\tilde{\pi}} = 110$  GeV (i.e.  $m_{\tilde{\rho}} = 830$  GeV). This is below the dijet constraints of [14] as can be seen also from figure 2.

At Tevatron energies, one also needs to consider pair production of  $\tilde{\pi}$ , however note that even though we expect  $2m_{\tilde{\pi}} < m_{\tilde{\rho}}$ ,  $\tilde{\pi}$  pair production is a 2-2 process in contrast to resonant  $\tilde{\rho}$  production which both reduces the cross section and leads to a variation of  $\sqrt{\hat{s}}$  from event to event, thereby decreasing the significance of any excess in kinematic distributions. Therefore, we do not expect the search strategy outlined in section 5 to yield as high a significance for this process.

It is intriguing to contemplate how light a  $\tilde{\pi}$ -mass can be accommodated, as  $\tilde{\pi}$  couples only to gluons in the SM, thus most existing experimental bounds are irrelevant. In this work we only consider  $m_{\tilde{\pi}} \gtrsim m_Z$  to avoid any constraints from corrections to the running of  $\alpha_s$ .

### 4.3 Other Sources of Potential Constraints

Since neither  $\tilde{\rho}$  nor  $\tilde{\pi}$  are electroweak charged, there are virtually no constraints on our benchmark model from LEP direct searches or precision electroweak data. Moreover, the fact that the  $\tilde{\rho}$ - $q$ - $\bar{q}$  coupling arises via  $\tilde{\rho}$ -gluon mixing makes the coloron coupling to quarks flavor blind, therefore there are no constraints from flavor changing processes on our benchmark model.

There are also no constraints from quark compositeness [30]. This is because compositeness bounds are sensitive to effective 4-fermion operators arising from integrating out heavy particles, however the range of coloron masses we consider is low enough for resonant production so the compositeness bounds are replaced by the constraints from dijet resonance searches, which are stronger.

One subtlety in our benchmark model is the existence of  $SU(3)_{\text{HC}}$  baryons, the lightest of which is a color octet, just like the lightest QCD baryons are arranged in an octet of flavor. Since hyper-baryon number  $U(1)_{\text{HB}}$  is exact in our benchmark model, the lightest hyper-baryon (LHB) is stable, while at collider time-scales the higher mass hyper-baryons decay promptly to the LHB. Once pair-produced, the LHB will hadronize with quarks or a gluon to form a color-singlet. In fact, the LHB has the same quantum numbers as a (Dirac) gluino, and thus the limits on stable gluinos cited in [31] apply. Based on the close analogy between QCD and hyper-color,  $m_{\text{LHB}} \gtrsim m_{\tilde{\rho}}$  holds, thus hyper-baryon pair production is compatible with the bounds listed in [31] for the range of parameters we consider in this work. We should note however, that it is straightforward to include additional particle content with renormalizable couplings which causes the hyper-baryons to decay unobservably into SM singlets plus jets at the Tevatron.

## 5. Discovery Potential at the Tevatron

Now that we have argued that our benchmark model is not ruled out by existing experimental constraints, one may worry that it is simply not visible in any channel, and hence not discoverable. This section will be aimed at showing that this is not at all the case and that the Tevatron has a strong discovery potential for our benchmark model within a broad range of parameters.

We will be concentrating in our search strategy on the production of the  $\tilde{\rho}$  particle, which is resonantly produced and dominantly decays to a pair of  $\tilde{\pi}$ , which then decay to two pairs of gluons. Thus the background to consider is the 4-jet QCD background, which is both quite large in cross section and has larger uncertainties compared to electroweak backgrounds. Fortunately there is one fact that favors signal over background for the range of  $\tilde{\rho}$  masses we are considering, namely that the signal is produced from a  $q$ - $\bar{q}$  initial state while the background is dominated by  $g$ - $g$  initiated processes, and the valence quark PDF's do not fall as rapidly as the gluon PDF's at intermediate to high  $x$  ( $x \gtrsim 0.2$ ). In any case, we will be conservative in our analysis of signal significance estimates considering the uncertainties in background and we will look for evidence that manifests itself as shape differences in

kinematic distributions, in contrast to an excess in overall normalization. Anticipating an unknown  $k$ -factor in the background we will use  $2 \text{ fb}^{-1}$  of background in all our analyses even though we only use  $1 \text{ fb}^{-1}$  of signal. We will use a simple  $\chi^2$  analysis to estimate the statistical significance of any excess, given by

$$(\text{stat. sig.})^2 = \sum_{\text{bins}} \left( \frac{n_s}{\sqrt{n_b}} \right)^2 \quad (5.1)$$

where the sum extends over the entire distribution and bin size is chosen to be smaller than any kinematic features of the distribution but large enough to contain many events.

Once again in the spirit of being conservative we limit our detailed studies to a region of parameter space where colorons are copiously produced, as our main goal is to prove discoverability as well as to lay out a general search strategy. A detailed study conducted by experimentalists using more sophisticated tools and statistical measures defining the limit of what is discoverable would be essential in producing concrete exclusion limits in the event of non-discovery. As a case study we will use our benchmark model with two choices for the mass of the coloron, the first being relatively light with  $m_{\tilde{\rho}} = 350 \text{ GeV}$  (where we take  $m_{\tilde{\pi}} = 100 \text{ GeV}$ ) and the second one being heavier with  $m_{\tilde{\rho}} = 600 \text{ GeV}$  (where we take  $m_{\tilde{\pi}} = 180 \text{ GeV}$ ). Colorons significantly lighter or heavier than these two cases are more challenging for discovery for reasons mentioned in our conclusions.

In contrast to the background, where the jet energies in an event are usually hierarchical, we expect all four jets in signal events to have similar energies. Therefore it appears plausible that a large cut on the  $p_T$  of all four jets should reduce background more than signal, with the further advantage that the perturbative QCD approximation employed in Monte Carlo simulations are more reliable for larger values of  $p_T$ . Moreover, for any realistic study we have to take into account the triggers used in the Tevatron analysis in order to ensure that all events in our signal and background samples are guaranteed to have been triggered on. To avoid issues with prescaled triggers we therefore will demand that all events used in our analysis have at least one jet with  $p_T \geq 120 \text{ GeV}$ , thereby making certain that they would have passed the  $100 \text{ GeV}$  single jet trigger used in CDF [32].

To simulate signal we use MadGraph version 4.2.3 [24] where we implement  $\tilde{\rho}, \tilde{\pi}$  and their relevant couplings to the SM using the provided user-mode. We generate signal for an integrated luminosity of  $1 \text{ fb}^{-1}$  using the process  $p\bar{p} \rightarrow \tilde{\pi}\tilde{\pi}$ . We then use the Pythia-PGS interface [24], where Pythia decays the  $\tilde{\pi}$  into a pair of gluons, provides the parton shower and hadronization, and PGS is used for jet reconstruction. We use the standard CDF parameter card supplied with the distribution, but use cone jets with  $\Delta R = 0.7$  in the reconstruction. For background, we generate parton level events with MadEvent using the process  $p\bar{p} \rightarrow jjjj$ , and again use the Pythia-PGS interface with the same parameters as for the signal.

### 5.1 Lighter Coloron Case, $m_{\tilde{\rho}} = 350 \text{ GeV}$

For this choice of mass, we find the production cross section of the coloron to be  $1.14 \times 10^2 \text{ pb}$ , however only a fraction of signal passes the leading jet  $p_T$  cut of  $120 \text{ GeV}$  we are using to

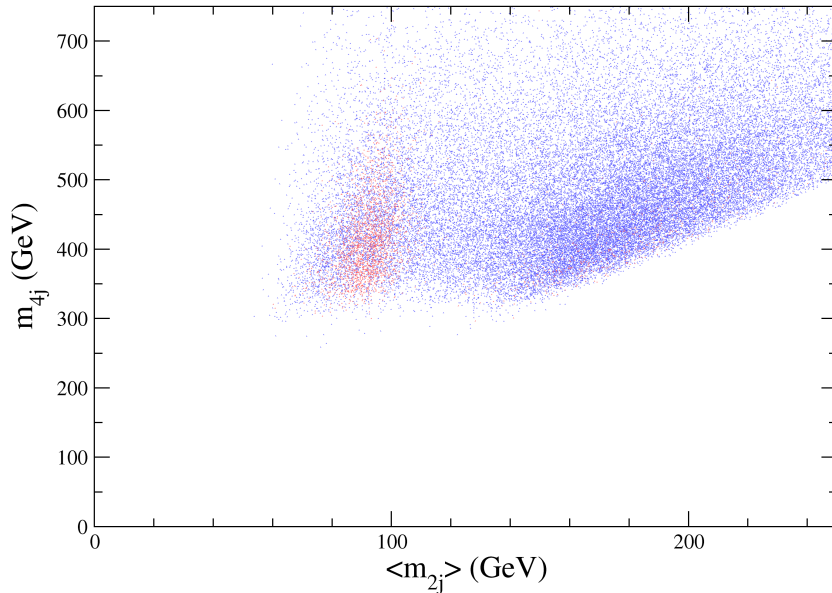


**Figure 4:** Dedicated coloron search in the benchmark model with  $m_{\tilde{\rho}} = 350$  GeV and  $m_{\tilde{\pi}} = 100$  GeV at Tevatron Run-II. We select events with at least one jet with  $p_T > 120$  GeV and four jets with  $p_T > 40$  GeV and we demand further that the four jets can be paired such that the invariant mass of the pairs is within 25 GeV of each other. We then plot the average pair invariant mass versus the 4j invariant mass. Each red dot represents a signal event which passed the cuts for  $1 \text{ fb}^{-1}$  of integrated luminosity while each blue dot represents a background event which passed the cuts for  $2 \text{ fb}^{-1}$  of integrated luminosity. The red dots along the diagonal are mispaired signal events, while most signal events are correctly paired and cluster near the true value of  $(m_{\tilde{\pi}}, m_{\tilde{\rho}})$ .

emulate the trigger, therefore we cannot afford to make too many other harsh cuts. We choose to veto events which have less than 4 jets with  $p_T$  greater than 40 GeV. After these cuts, we find  $\sigma_s = 3.60$  pb while  $\sigma_b = 65.8$  pb.

To exploit the full kinematic information present in the signal we further pair the four leading jets into two pairs and veto all events where no possible pairing yields two pairs with  $m_{\text{inv}}$  within 25 GeV of each other. (If there is more than one such possible pairing, we take the one that yields the closest  $m_{\text{inv}}$  for the pairs.) This further reduces the signal cross section to 2.66 pb and the background to 20.8 pb. We then plot the average invariant mass of the two pairs against the invariant mass of the four leading jets. (A similar search strategy relying on the pairing of four jets was used in [33] albeit without the additional advantage of the presence of a primary four jet resonance.) The results are plotted in figure 4 where the shape difference between the signal and background is very clearly visible. Most signal points are correctly paired and accumulate in a small region close to the actual masses of the  $\tilde{\rho}$  and

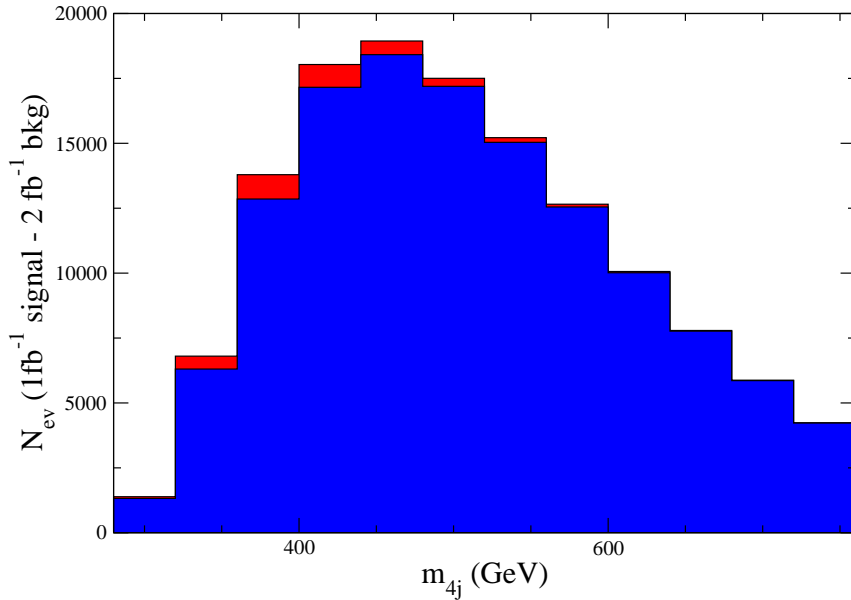


**Figure 5:** More general coloron resonance search in the 4j channel at Tevatron Run-II. In events with at least one jet with  $p_T > 120$  GeV and four jets with  $p_T > 40$  GeV we plot the invariant mass of the four leading jets. Blue corresponds to  $2 \text{ fb}^{-1}$  of background while red corresponds to  $1 \text{ fb}^{-1}$  of signal for  $m_{\tilde{\rho}} = 350$  GeV.

$\tilde{\pi}$  while some signal events are mispaired and appear scattered in a larger region along the diagonal where the background is most densely populated. We find the statistical significance of the excess to be  $32.3\sigma$ . Even though we are aware that there are sources of systematic error that are not accounted for in our analysis, this result is strong enough to indicate that such a search strategy will yield definitive results even when done with more sophisticated tools such as a fully realistic detector simulation and taking into account shape dependent corrections or further subtleties involved in a real experimental analysis.

In fact, with such high signal significance it is interesting to attempt a less model dependent search that would have reduced sensitivity, which however may be sensitive to models other than our benchmark, e.g. when the coloron decays to two particles of unequal mass. Therefore we try to be as inclusive as possible and determine whether a search that was not optimized to look for secondary resonances would still discover the coloron. Using the same  $p_T$  cuts as above but without pairing up the jets we simply construct the invariant mass of the leading four jets. The results are displayed in figure 5. The significance of the excess in this distribution is  $13.4\sigma$ . In order to reduce any bias in the first few bins introduced by analysis cuts we repeat the analysis where we disregard any discrepancy in the bins up to

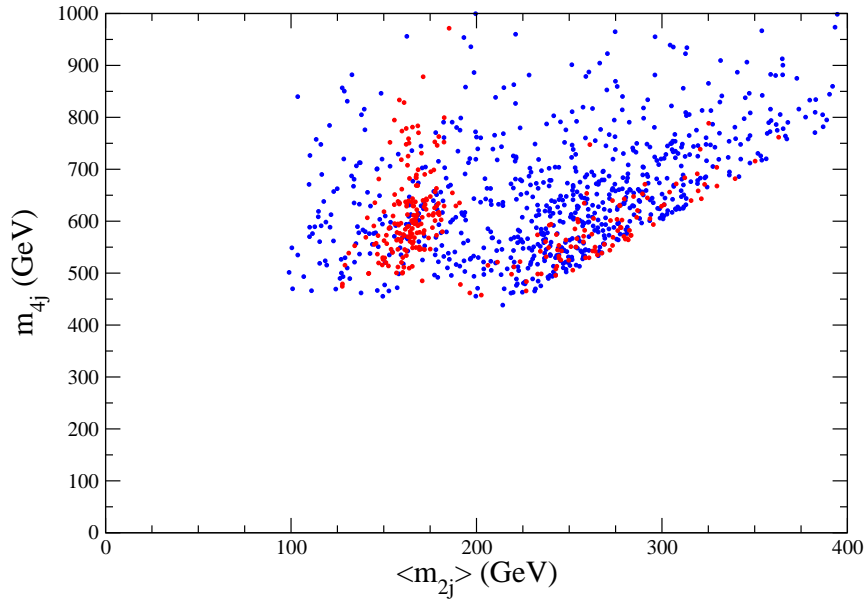


**Figure 6:** Dedicated coloron search in the benchmark model with  $m_{\tilde{\rho}} = 600$  GeV and  $m_{\tilde{\pi}} = 180$  GeV at Tevatron Run-II. We select events with at least one jet with  $p_T > 120$  GeV and four jets with  $p_T > 90$  GeV and we demand further that the four jets can be paired such that the invariant mass of the pairs is within 25 GeV of each other. We then plot the average pair invariant mass versus the 4j invariant mass. Each red dot represents a signal event which passed the cuts for  $1 \text{ fb}^{-1}$  of integrated luminosity while each blue dot represents a background event which passed the cuts for  $2 \text{ fb}^{-1}$  of integrated luminosity.

$m_{\text{inv}} = 400$  GeV and still find a significance of  $8.3\sigma$ .

Even though these results seem to suggest that an almost blind search could provide initial evidence for the existence of a colored resonance decaying to a four jet final state, one needs to worry that corrections in the calculation of the background can give rise to a shape difference large enough to nullify the significance of the excess in this more general search. This situation cannot be improved greatly in looking for the lighter coloron, since we cannot make our  $p_T$  cuts much harder without losing the signal. We will come back to this issue in the study of the heavier coloron however, and argue that the prospects are much better in that case.

## 5.2 Heavier Coloron Case, $m_{\tilde{\rho}} = 600$ GeV

Having shown that even a coloron as light as 350 GeV can be discovered despite trigger inefficiencies for the signal as well as higher backgrounds, we now study the case of a heavier coloron with  $m_{\tilde{\rho}} = 600$  GeV which has a production cross section of 10.0 pb at Run-II. For



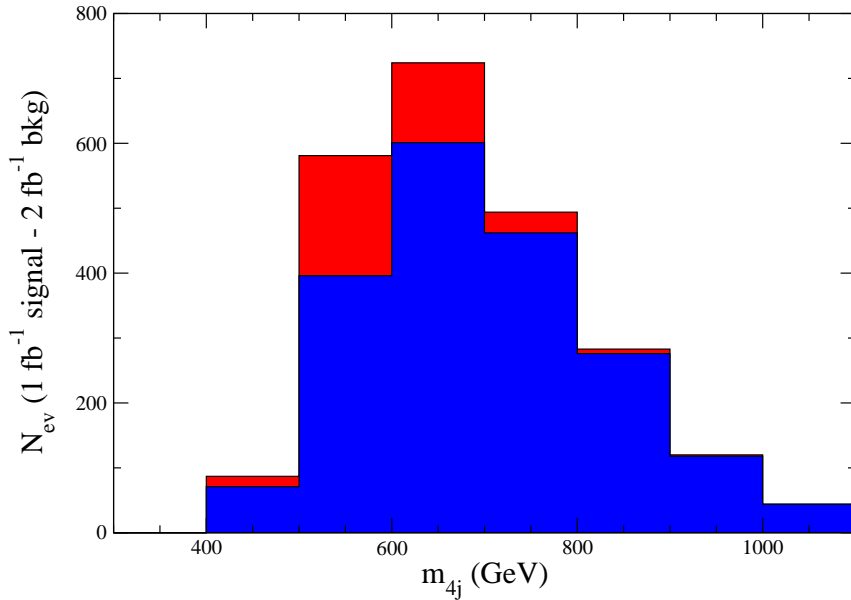


**Figure 7:** More general coloron resonance search in the 4j channel at Tevatron Run-II. In events with at least one jet with  $p_T > 120$  GeV and four jets with  $p_T > 90$  GeV we plot the invariant mass of the four leading jets. Blue corresponds to  $2 \text{ fb}^{-1}$  of background while red corresponds to  $1 \text{ fb}^{-1}$  of signal for  $m_{\tilde{\rho}} = 600$  GeV.

this case, most signal events automatically have a leading jet with  $p_T \geq 120$  GeV and we can afford to put a harder cut on the  $p_T$  of the other jets. In fact we will choose to accept events in our analysis which have at least four jets with  $p_T \geq 90$  GeV. After these cuts, the signal and background cross sections are  $\sigma_s = 0.36$  pb and  $\sigma_b = 0.99$  pb. As before, we veto events in which the leading four jets cannot be paired in a way to give two pairs with invariant masses within 25 GeV of each other, which further reduces the cross section after cuts to  $\sigma_s = 0.27$  pb and  $\sigma_b = 0.38$  pb. The results are displayed in figure 6 where the significance of the excess is  $17.2\sigma$ .

As before, we also perform a less model dependent search looking at the invariant mass of the four leading jets using the same cuts as above but without demanding that they can be paired. The results are displayed in figure 7 where the statistical significance of the excess is  $10.8\sigma$ . Coming back to the issue of shape dependent corrections to the background we note that these are events where there are four very hard jets which are maximally separated from each other, which is where we expect the perturbative expansion to be most reliable. Keeping in mind that we are already using twice as much background as signal, it would require nearly a 100% error on the shape of the background to eliminate the significance of the signal excess

in the case of the heavier coloron.

## 6. Concluding Remarks

We have emphasized in this paper how a variety of new physics scenarios can lead to the existence of a massive color octet vector meson, the coloron. We have used an analogy to QCD to set up a benchmark model of a composite coloron and write a phenomenological Lagrangian for it, where our choices for the values of the couplings are simply extrapolated from hadronic data. We have then shown that this benchmark model with new colored states at a few hundred GeV is fully consistent with to-date experimental bounds and have outlined a promising search strategy at the Tevatron for discovering these states using already existing data.

The range of coloron mass to which the Tevatron is sensitive can be understood as follows: If the coloron mass is too low (below about 300 GeV), then the signal events will not pass the single-jet trigger mentioned in section 5 while prescaled triggers with lower thresholds would severely reduce the signal significance. For coloron masses that are too large, the cross section drops below levels needed for discovery, for instance above 850 GeV the cross section drops below 1 pb which in our analysis would lead to a few tens of events after kinematic cuts. Exact limits on the discovery reach will depend on a careful estimation of background, a realistic treatment of detector effects as well as a careful statistical definition of what is discoverable, which should be part of a detailed study conducted by experimentalists. In this paper we have adopted a conservative view of focusing attention on two choices for the coloron mass ( $m_{\tilde{\rho}} = 350$  GeV and  $m_{\tilde{\rho}} = 600$  GeV in the benchmark model) where we demonstrated a strong potential for discovery even with the above mentioned uncertainties taken into account.

It is worth considering how the collider phenomenology is affected by the value of the ratio  $m_{\tilde{\pi}}/m_{\tilde{\rho}}$ . This ratio is fixed in the benchmark model, but in the spirit of (3.10) being an effective Lagrangian we can view  $m_{\tilde{\pi}}$  as an independent parameter. Including input masses for the hyper-quarks in (2.1) can increase  $m_{\tilde{\pi}}/m_{\tilde{\rho}}$  above 0.3, its value in the benchmark model. Hyper-quark masses that are comparable in magnitude to  $\Lambda_{HC}$  will cause the  $\tilde{\rho} \rightarrow \tilde{\pi}\tilde{\pi}$  decay channel to become kinematically inaccessible, therefore this possibility is ruled out by the dijet resonance constraints, on the other hand a modest increase in  $m_{\tilde{\pi}}/m_{\tilde{\rho}}$  will not significantly affect our analysis methods. Smaller  $\tilde{\pi}$  masses cannot be obtained from the microscopic theory (2.1) and even in the phenomenological model (3.10) the benchmark value of  $m_{\tilde{\pi}}$  is the technically natural one. If  $m_{\tilde{\pi}}$  in (3.10) was tuned to a smaller value, one would expect the pairs of jets resulting from the  $\tilde{\rho}$  decay to become more collinear, not only leading to a smaller efficiency in observing four separated hard jets and making discovery more difficult, but in the extreme limit causing signal events to be reconstructed as having two back-to-back jets, thereby conflicting with dijet resonance bounds.

We would like to elaborate on the point that the Tevatron is the ideal place to look for a coloron, and that the LHC will have lessened sensitivity to a signal of this kind. One reason is simply that the LHC, being a  $p$ - $p$  collider, will suffer from a suppression in the cross section of

a resonance produced from a  $q\bar{q}$  initial state especially for TeV scale masses. The lower mass ranges we considered in this paper would face severe backgrounds at the LHC considering that the gluon PDF's would be sampled at much lower  $x$ . Furthermore, the increased number of events per bunch crossing due to higher luminosity as well as the higher trigger thresholds will make event selection much more difficult for the LHC environment. On the other hand, it would be interesting to assess the reach of the LHC for other states appearing in the theory such as the hyper-baryon of our model, which can decay to SM singlets plus jets, thereby leading to missing energy signatures, or even be stable at collider time-scales in which case it would be challenging to distinguish it from a stable gluino.

In this paper, the coupling of the coloron to ordinary quarks is inherited entirely via gluon-coloron mixing. This ensured compatibility of the new physics with a variety of precision tests, even for relatively low coloron mass. One can generalize this set-up to include direct couplings of the coloron (and/or secondary resonances) to quarks, either continuing in a flavor-blind manner [4], or flavor-dependently (in particular with large top coupling) as motivated by some approaches to the Hierarchy Problem [1]. When such direct couplings are significant, the coloron mass is forced above about a TeV in order to avoid constraints from some combination of low-energy precision tests, dijet searches, and studies of top production. That is, the coloron is effectively pushed outside the Tevatron window. However the direct couplings can then help compensate for some of the difficulties associated with LHC discussed in the preceding paragraph, enabling discovery as dijet or top-antitop resonances, or in heavy flavor decays of secondary resonances. In this sense, the scenario discussed in the present paper and its Tevatron signatures is complementary to the case of significant direct coloron-quark couplings and their LHC phenomenology.

Existing theoretical models occupy only a subset of possible phenomenological coloron parameters. Whether a coloron has a deep connection to the (resolution of the) Hierarchy Problem or not, we cannot in generality predict the strength and flavor-dependence of coloron-quark couplings. While different limits have now been studied theoretically, it may be that in an intermediate situation data from both the Tevatron and the LHC, in jets as well as more distinctive channels such as heavy flavors or even missing energy, may prove essential in uncovering the physics of the coloron.

## Acknowledgments

We would like to thank Johan Alwall for his infinite patience and help using MadEvent, Morris Swartz for invaluable discussions and advice, Sarah Eno, Isaac Hall, Robert Harris, Kenichi Hatakeyama, Joey Huston, and Petar Maksimovic for assistance with experimental issues, Sekhar Chivukula, Bogdan Dobrescu, David E. Kaplan, Steve Mrenna, Matthew Schwartz, John Terning and Brock Tweedie for useful insights, Henry Tye for pointing out to us the three-jet decay mode of the coloron, and Bruce Knuteson for helping us with issues concerning Tevatron global searches. The authors are supported by the National Science Foundation grant NSF-PHY-0401513 and by the Johns Hopkins Theoretical Interdisciplinary Physics and

Astrophysics Center. C.K. and T.O. are further supported in part by DOE grant DE-FG02-03ER4127 and by the Alfred P. Sloan Foundation. T.O. is also supported by the Maryland Center for Fundamental Physics.

## References

- [1] C. T. Hill, Phys. Lett. B **266**, 419 (1991).
- [2] E. Farhi and L. Susskind, Phys. Rev. D **20**, 3404 (1979).
- [3] S. Cullen, M. Perelstein and M. E. Peskin, Phys. Rev. D **62**, 055012 (2000) [arXiv:hep-ph/0001166].
- [4] R. S. Chivukula, A. G. Cohen and E. H. Simmons, Phys. Lett. B **380**, 92 (1996) [arXiv:hep-ph/9603311].
- [5] E. H. Simmons, Phys. Rev. D **55**, 1678 (1997) [arXiv:hep-ph/9608269].
- [6] D. Choudhury, R. M. Godbole, R. K. Singh and K. Wagh, Phys. Lett. B **657**, 69 (2007) [arXiv:0705.1499 [hep-ph]].
- [7] C. T. Hill and S. J. Parke, Phys. Rev. D **49**, 4454 (1994) [arXiv:hep-ph/9312324].
- [8] D. A. Dicus, B. Dutta and S. Nandi, Phys. Rev. D **51**, 6085 (1995) [arXiv:hep-ph/9412370].
- [9] R. Casalbuoni, P. Chiappetta, D. Dominici, A. Fiandrino and R. Gatto, Z. Phys. C **69**, 519 (1996) [arXiv:hep-ph/9505212].
- [10] K. Agashe, A. Belyaev, T. Krupovnickas, G. Perez and J. Virzi, Phys. Rev. D **77**, 015003 (2008) [arXiv:hep-ph/0612015]; B. Lillie, L. Randall and L. T. Wang, JHEP **0709**, 074 (2007) [arXiv:hep-ph/0701166].
- [11] B. Lillie, J. Shu and T. M. P. Tait, arXiv:0712.3057 [hep-ph].
- [12] M. Guchait, F. Mahmoudi and K. Sridhar, arXiv:0710.2234 [hep-ph].
- [13] J. Alitti *et al.* [UA2 Collaboration], Nucl. Phys. B **400**, 3 (1993).
- [14] F. Abe *et al.* [CDF Collaboration], Phys. Rev. D **55**, 5263 (1997) [arXiv:hep-ex/9702004]; V. M. Abazov *et al.* [D0 Collaboration], Phys. Rev. D **69**, 111101 (2004) [arXiv:hep-ex/0308033]; CDF Collaboration, CDF public note 9246 [publication in preparation].
- [15] F. Abe *et al.* [CDF Collaboration], Phys. Rev. Lett. **82**, 2038 (1999) [arXiv:hep-ex/9809022].
- [16] L. Susskind, Phys. Rev. D **20**, 2619 (1979); S. Weinberg, Phys. Rev. D **13**, 974 (1976); S. Weinberg, Phys. Rev. D **19**, 1277 (1979).
- [17] M. J. Strassler and K. M. Zurek, Phys. Lett. B **651**, 374 (2007) [arXiv:hep-ph/0604261].
- [18] J. Kang and M. A. Luty, arXiv:0805.4642 [hep-ph].
- [19] E. Eichten, I. Hinchliffe, K. D. Lane and C. Quigg, Rev. Mod. Phys. **56**, 579 (1984) [Addendum-ibid. **58**, 1065 (1986)].
- [20] K. Lane and S. Mrenna, Phys. Rev. D **67**, 115011 (2003) [arXiv:hep-ph/0210299].
- [21] A. R. Zerwekh and R. Rosenfeld, Phys. Lett. B **503**, 325 (2001) [arXiv:hep-ph/0103159].

- [22] A. Manohar and H. Georgi, Nucl. Phys. B **234**, 189 (1984).
- [23] H. Georgi, *Menlo Park, Usa: Benjamin/cummings ( 1984) 165p*
- [24] J. Alwall *et al.*, JHEP **0709**, 028 (2007) [arXiv:0706.2334 [hep-ph]]; T. Sjostrand, S. Mrenna and P. Skands, JHEP **0605**, 026 (2006) [arXiv:hep-ph/0603175]; J. Conway *et al.*, <http://www.physics.ucdavis.edu/~conway/research/software/pgs/pgs4-general.htm>; E. Boos *et al.* [CompHEP Collaboration], Nucl. Instrum. Meth. A **534**, 250 (2004) [arXiv:hep-ph/0403113].
- [25] T. Aaltonen *et al.* [CDF Collaboration], arXiv:0709.0705 [hep-ex].
- [26] F. Abe *et al.* [CDF Collaboration], Phys. Rev. D **54**, 4221 (1996) [arXiv:hep-ex/9605004].
- [27] T. Aaltonen *et al.* [CDF Collaboration], arXiv:0712.1311 [hep-ex].
- [28] H. L. Lai *et al.* [CTEQ Collaboration], Eur. Phys. J. C **12**, 375 (2000) [arXiv:hep-ph/9903282].
- [29] E. L. Berger and M. Jacob, Phys. Lett. B **147**, 197 (1984).
- [30] I. Bertram and E. H. Simmons, Phys. Lett. B **443**, 347 (1998) [arXiv:hep-ph/9809472].
- [31] A. Mafi and S. Raby, Phys. Rev. D **62**, 035003 (2000) [arXiv:hep-ph/9912436].
- [32] A. Abulencia *et al.* [CDF - Run II Collaboration], Phys. Rev. D **75**, 092006 (2007) [Erratum-ibid. D **75**, 119901 (2007)] [arXiv:hep-ex/0701051].
- [33] R. S. Chivukula, M. Golden and E. H. Simmons, Nucl. Phys. B **363**, 83 (1991).